ATTACHMENT 11

16

Density Structures in "Low Inflow Estuaries"

John L. Largier, Clifford J. Hearn, and D. Bart Chadwick

Abstract

The study of estuarine hydrodynamics has been dominated by a focus on the defining feature of estuaries - freshwater inflow. Low-inflow "estuaries" (LIE's), or semi-enclosed bays, have received very little attention in spite of their common occurrence. In this paper, we discuss the occurrence of LIE's as a seasonal feature in mediterranean-climate regions (e.g., California, USA). Buoyancy fluxes are dominated by air-water exchange. There is competition between a positive buoyancy flux due to heating and a negative buoyancy flux due to evaporation. In spite of large thermohaline signals, the resultant buoyancy flux is often too weak to bring about vertical stratification and buoyancy-driven exchange in shallow estuarine basins. This results in very long residence times being observed in tidally sheltered waters, such as at the landward end of these LIE basins. Through a simple model of surface fluxes and longitudinal dispersion in LIE's, we explain observed temperature, salinity and density structures in Tomales, San Diego, and Mission Bays (California, USA). In summary, we identify four regions: a marine region in the outer bay (dominated by tidal exchange with the ocean), a thermal region (where heating dominates the buoyancy flux), a hypersaline region (where evaporation dominates the buoyancy flux), and an estuarine regime (where freshwater inflow dominates the buoyancy flux). The clear spatial separation of thermal and hypersaline regimes is owing to the different temporal structure of heating and evaporation in mediterranean-climate estuaries.

Introduction

In much the same way that people who study rivers in arid or semi-arid areas refer to them as water courses, recognizing that run-off is not persistent, so we too need to find a new term or re-define the old one (e.g., Pritchard, 1967) to allow for the fact that many "estuaries" do not experience a persistent freshwater inflow. In arid areas, or during the dry season in mediterranean climate regions, river inflow is negligible or absent. Any estuary-ocean density differences are due to differential heating or evaporation, i.e., due to surface buoyancy fluxes. With the anthropogenic extraction of water from rivers, more estuaries are becoming net evaporative during the dry season (i.e., the fresh water loss from the basin is greater than that supplied by river inflow).

Observations from three Californian estuaries represent the essential spatio-temporal density structures during dry mediterranean-climate summers. However, limited published data from estuaries in other mediterranean regions suggest that the structures observed in California are likely to be found in many of the estuaries of southwestern Australia, southwestern South Africa, Portugal, Morocco, Chile, northwestern Mexico, and so on.

In the following, a simplified estuarine basin is considered (Fig. 1). This basin receives freshwater via river inflow R and precipitation P while it loses freshwater through evaporation E. Heat is exchanged with the atmosphere (heat flux Q). The temperature, salinity and density of this basin depends on the strength of these inputs/outputs and on the rate of hydrodynamic exchange

Buoyancy Effects on Coastal and Estuarine Dynamics
Coastal and Estuarine Studies Volume 53, Pages 227-241

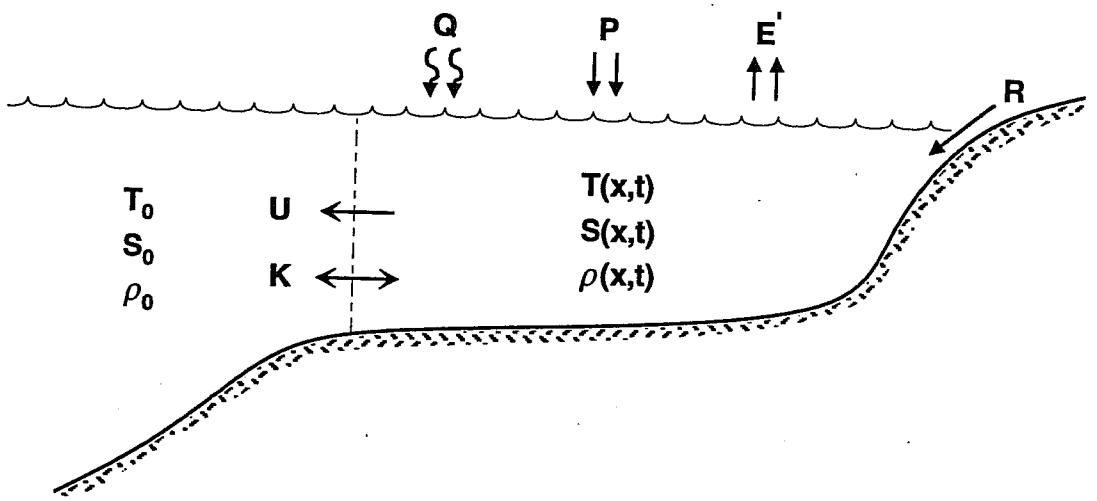

Figure 1. Schematic and definition of significant water and heat exchanges in a low-inflow estuary (variables defined in text).

with the adjacent ocean (the ambient). This hydrodynamic exchange is expressed as the sum of subtidal advection U and subtidal diffusion K. Following Largier et al. (1996), the basin is considered to be a "hypersaline estuary" if its salinity is significantly greater than the ocean salinity (i.e., exceeds ocean salinity by at least one standard deviation of ocean salinity fluctuations). A "thermal estuary" describes a basin in which the density structure is dominated by temperature. An "inverse estuary" is one in which the density of the water exceeds that in the ocean.

Observations

Hypersaline conditions, a clear indicator of low freshwater inflow, have been observed in many estuaries along the Pacific coast of the Californias (Fig. 2). In Tomales Bay, the northernmost of these basins, temperature and salinity data have been collected over a 7-year period (Largier et al., 1996). The seasonal cycle is dramatic, dominating any interannual fluctuations (Fig. 3). Winters are cold and wet, yielding large river inflow and low salinities. Summers are warm and dry, resulting in net evaporation and high salinities. Occupying a rift valley along the San Andreas fault, this basin is long and thin. Temperature, salinity and density data are clearly functions of the distance from the ocean, at one end, and from the major river flowing in at the other end. At station 16, 16 km from the mouth and 4 km from the head, salinities drop into the mid-20's while temperatures drop below 10° C during winter. In summer, salinities exceed ocean values by about 2 and temperatures exceed ocean values by several degrees centigrade. While estuarine temperatures rise during early summer, ocean temperatures remain low as a result of wind-driven upwelling along the ocean coast (Lentz, 1991; Largier et al., 1993). The summer gradient in temperature maintains a positive density gradient (a "thermal estuary"). It is only in the fall, when estuary temperatures drop, that the density gradient approaches zero and may become inverse owing to the hypersalinity of the basin, which persists until the onset of winter rains.

The coarse temporal resolution of Tomales Bay data does not allow one to ascertain whether a steady state salt balance occurs during late summer. In Mission Bay, where data were collected more frequently, a quasi-steady salinity and temperature distribution is observable from June to September (Fig. 4). In this basin, hypersaline conditions are only observed in the one-dimensional side branches and not in the more complex morphology of the middle and outer bay (Fig. 2). As in

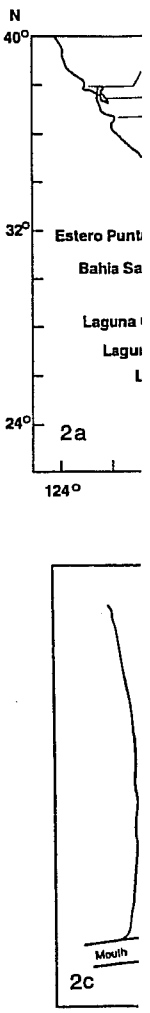

Figure 2. Se
systems in wl
region of hype
Bay stations a

Tomales Ba
the fall and
the temperat
This density
event in 19
by a seawar

A simi
longer syste
temperature
salinity don

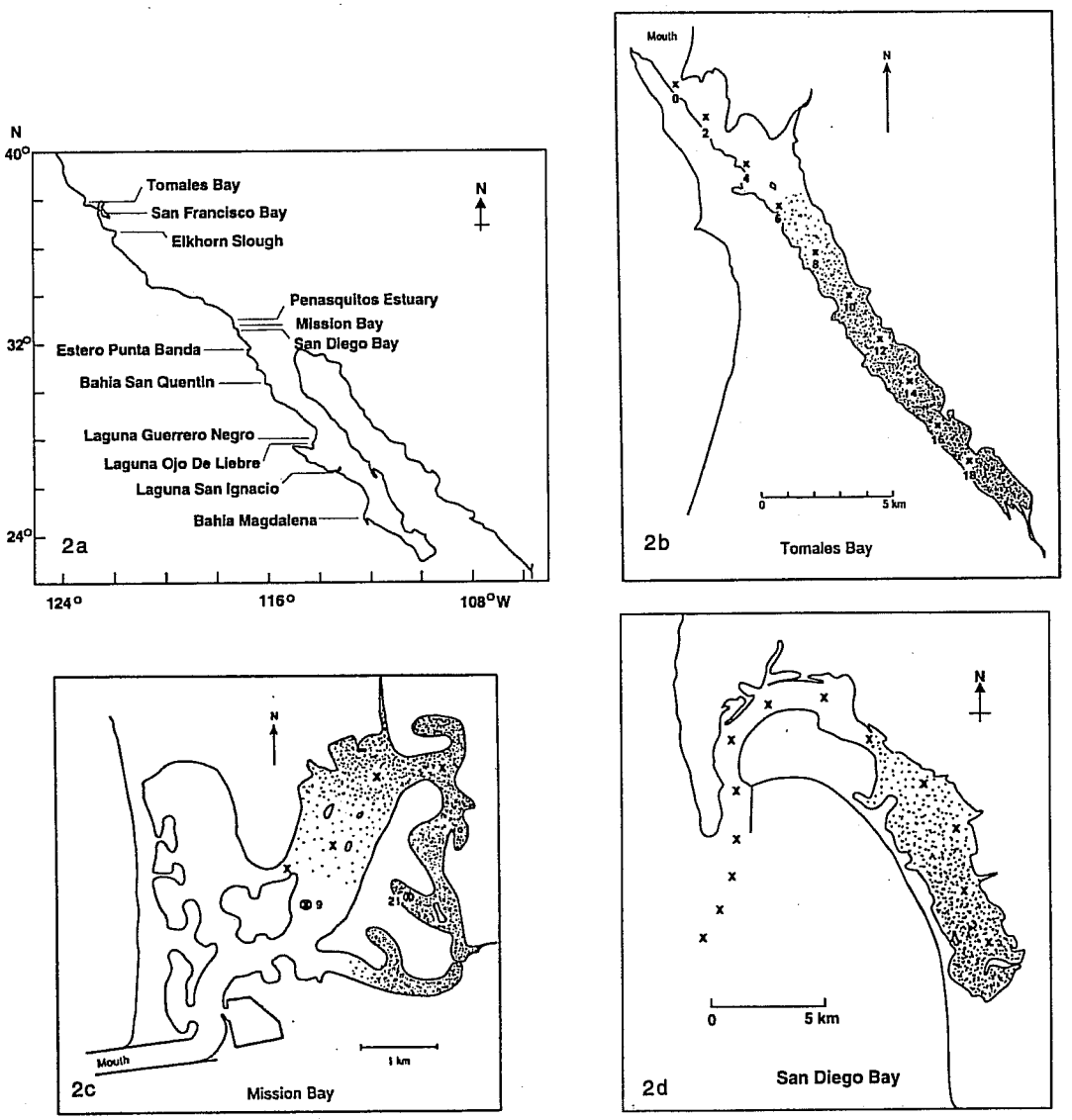

Figure 2. Seasonally hypersaline estuaries along the west coast of North America. (a) Location of various systems in which hypersalinity has been reported. (b) Position of CTD stations in Tomales Bay and typical region of hypersalinity in late summer (shaded). (c) Mission Bay stations and hypersaline region. (d) San Diego Bay stations and hypersaline regions.

Tomales Bay, inverse conditions are only observed following the decrease in water temperatures in the fall and early winter, prior to rainfall. In Mission Bay, the hypersalinity is stronger and when the temperature gradient reverses in early winter a significant inverse structure is observed (Fig. 4). This density head persists, however, indicating the absence of a singular density-driven flushing event in 1992. Rather, a steady salinity indicates that freshwater loss via evaporation is balanced by a seaward salt flux due to tidal diffusion mechanisms.

A similar seasonal cycle and longitudinal structure is observed in San Diego Bay. In this longer system (Figs. 2 and 5), one notices the separation between the region where increasing temperature dominates the density change ("thermal estuary") and the region where the increasing salinity dominates density change ("hypersaline estuary"). The middle and outer bay is thus

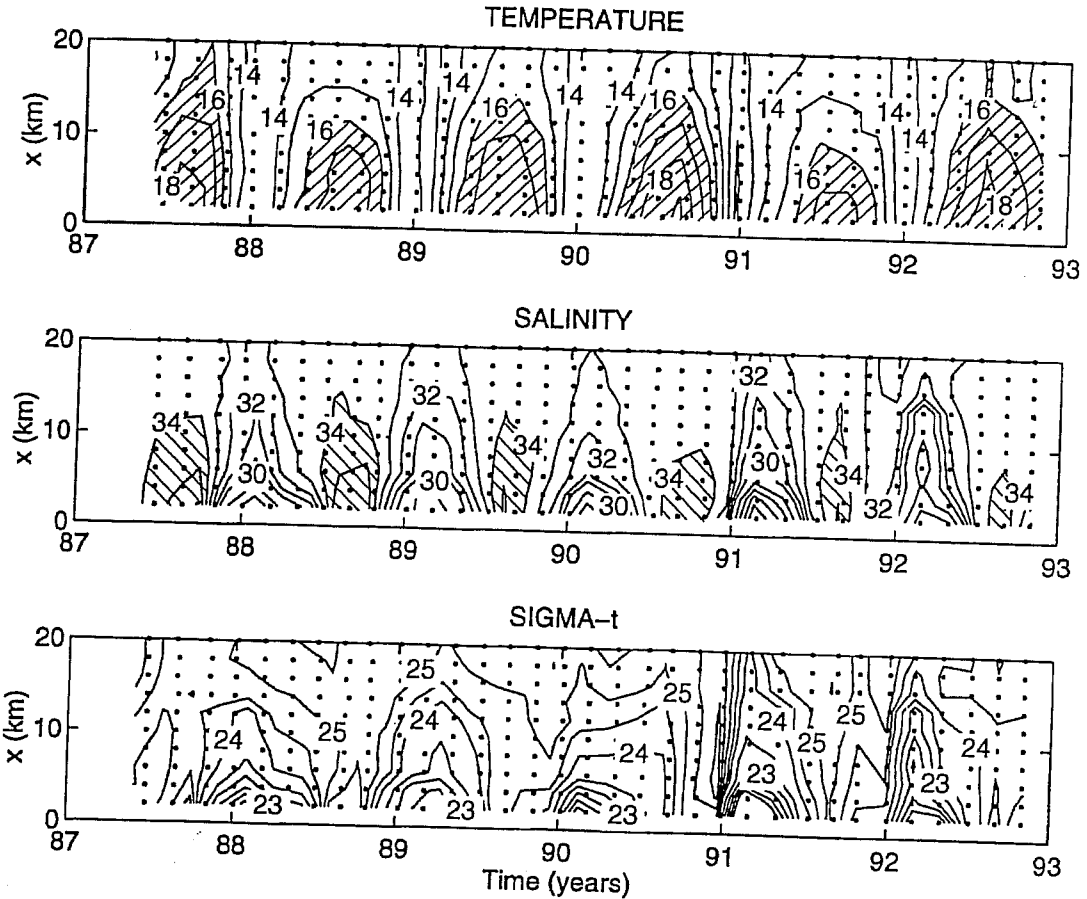

Figure 3. Multi-year seasonal variation of vertically averaged temperature, salinity, and sigma-t in Tomales Bay, as a function of distance from the head ($x=0$). Regions of water that are warmer and saltier than the ocean are hatched (summer). Regions of freshwater influence are seen in winter.

characterized by a positive density gradient while the innermost part of the bay is characterized by a negative density gradient ("inverse estuary"). A density minimum is found in between these outer and inner regions. Reviewing Tomales Bay and Mission Bay data a similar offset of temperature and salinity structures can be seen in the density structure (this is not clearly shown in this paper).

The Longitudinal Salt Balance

Noting the occurrence of hypersalinity in systems with long, narrow basins or in long, narrow branches of systems, Largier et al. (1996) use the following one-dimensional model of vertically averaged salinity to illustrate the essence of the subtidal salt balance of these low-inflow estuaries:

$$\partial_t S = \partial_x \left[\left[\frac{R}{wh} + \frac{Px}{h} - \frac{E'x}{h} \right] S - K \partial_x S \right] \qquad (1)$$

where h is the basin depth, w is the basin width, x is the longitudinal distance from the head of the estuary, t is time, K is the subtidal eddy diffusivity in the longitudinal direction and E', R and P are

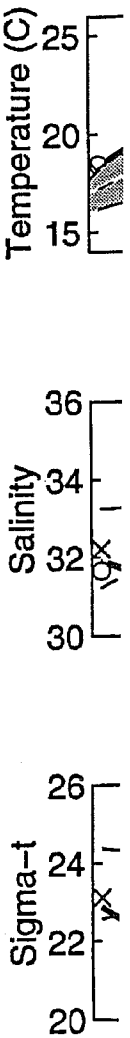

Figure 4. Th
from the ocea
(bold line) ar
extent of the
north of the m
the ocean is i
marks indicat

as earlier (F
distribution
longitudina
expression f

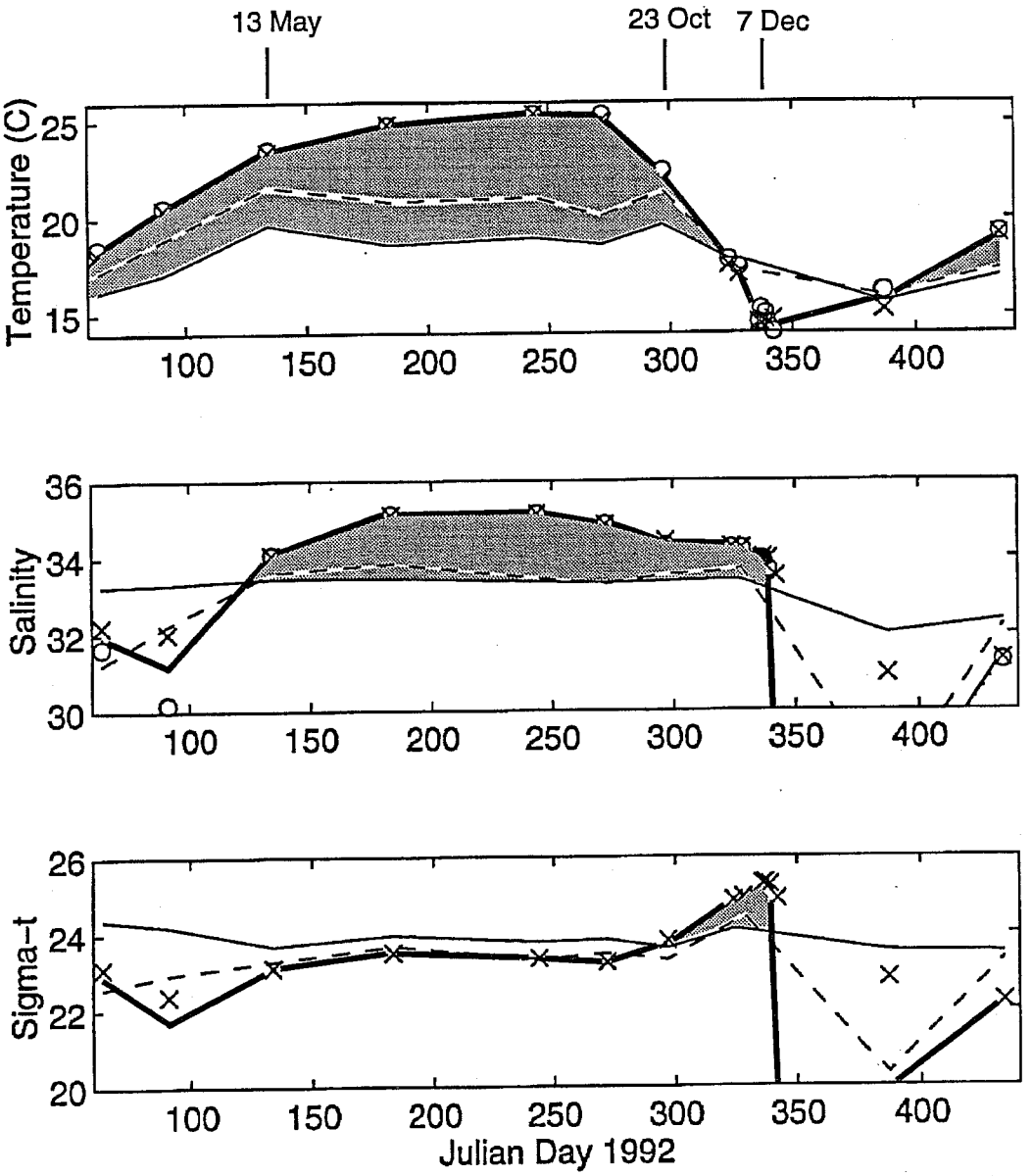

Figure 4. The seasonal variation in temperature, salinity, and sigma-t in Mission Bay. At station 21 (farthest from the ocean, Figure 2c), surface values (open circles), bottom values (crosses), and vertical average values (bold line) are plotted. For comparison, vertical average values are also plotted for station 9, at the landward extent of the well-flushed outer estuary (dashed line), and for Scripps Pier, an ocean station several kilometers north of the mouth of the Bay (solid line). The period during which station 21 is warmer, saltier or denser than the ocean is indicated by shading. Stratification is not observed in the hypersaline inner estuary. The date marks indicate the start and end of hypersaline and inverse conditions.

as earlier (Fig. 1). Using $E = E'\text{-}P\text{-}R/wx$ as net evaporation, and expecting a quasi-steady salinity distribution in mid-summer ($\partial_t S = 0$) one can solve for $S(x)$. In all three systems studied, longitudinal dispersion appears to be a continuous subtidal process. Using a mixing length expression for the longitudinal diffusivity $K=kx^2$, one obtains the solution

$$\frac{S}{S_0} = \left[\frac{x}{L}\right]^{-E/kH} \tag{2}$$

which fits well to observed data (e.g., San Diego Bay, Fig. 6). From the longitudinal salinity distribution one can estimate the average residence time of water at a particular distance from the ocean (assuming constant salinity S_0), using the bulk expression

$$\tau_{res} = \frac{(S - S_0)}{ES} h \tag{3}$$

Average residence times increase markedly towards the head of the basin with negligible inflow. This is consistent with the marked decrease in the value of the tidal diffusivity, $K=kx^2$, obtained from a mixing length model. This long residence, relative to the time scales of surface fluxes (e.g., evaporation), is the defining dynamical character of these hypersaline basins.

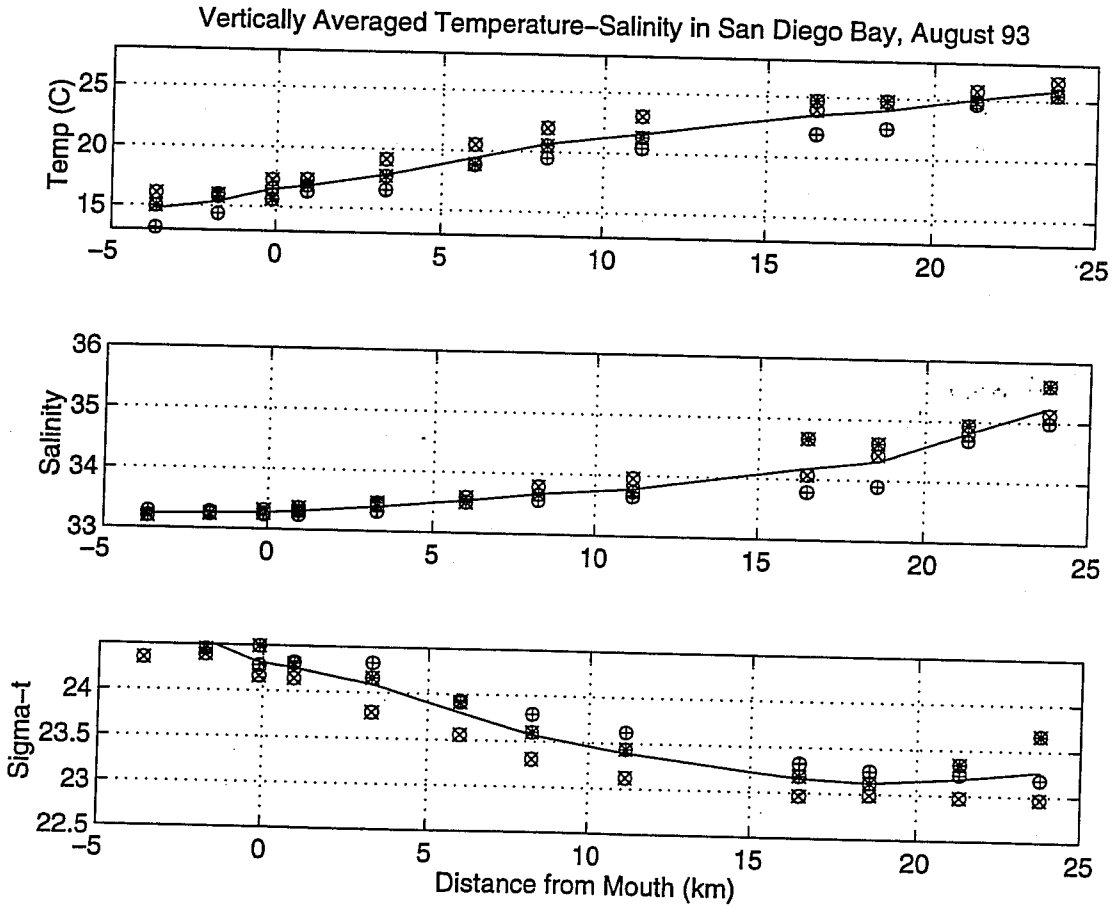

Figure 5. Vertically averaged temperature, salinity, and sigma-t for San Diego Bay on 3 days in August 1993 (symbols). Solid line is average of the three data sets, which exhibit tidal differences. Data are plotted as distance from the mouth.

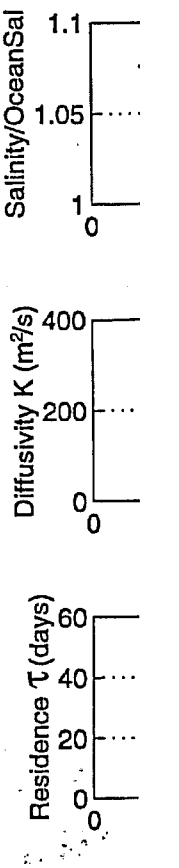

Figure 6. In t
averaged salir
function of dis
as asterisks ar
Largier et al.,

Largier
salinity distı
which are di
Residence ti

Surface E

While
structures ar
in salinity a
characterize
tropical sys
Wolanski, 1
there is no a
As not
the maximu

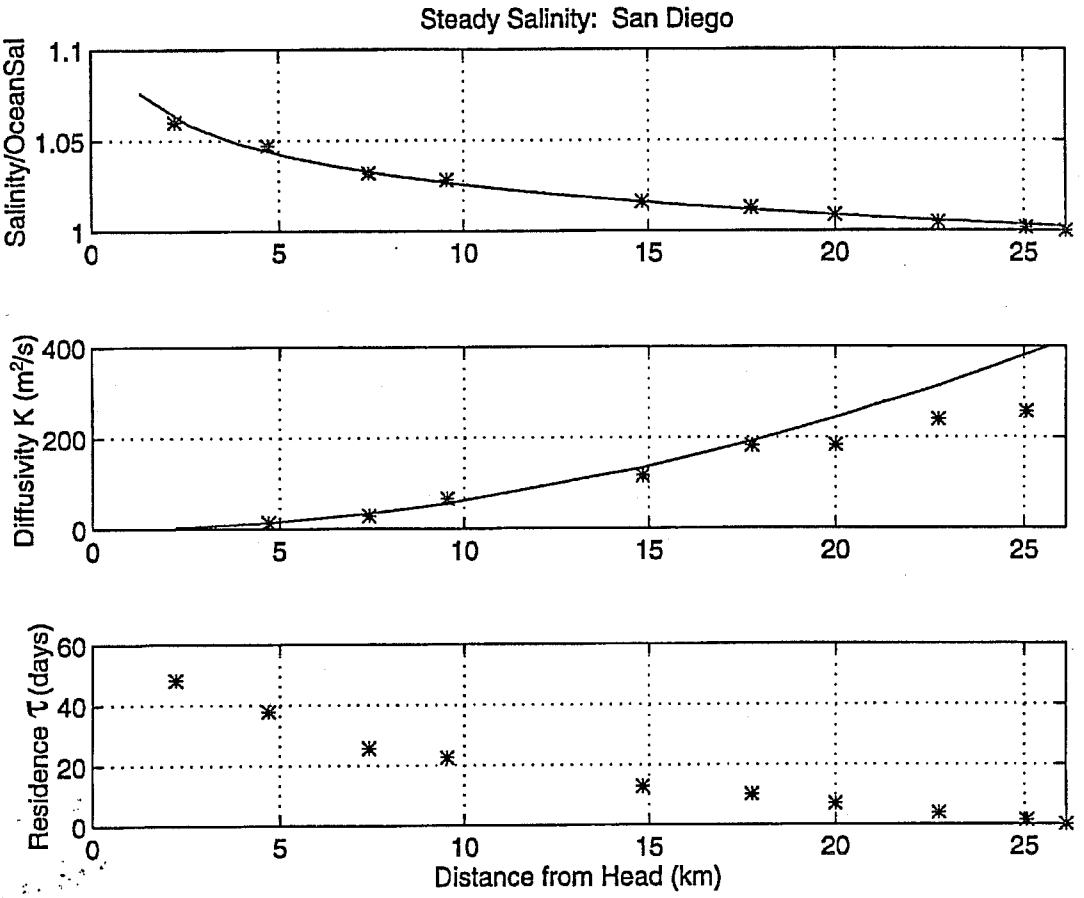

Figure 6. In the top panel, the solution from Eqn. (2), plotted as a solid line, is fitted to observed vertically averaged salinity (from line in Fig. 5.), plotted as asterisks. The middle panel presents diffusivity $K=kx^2$ as a function of distance from the head x, with the value of k obtained from the fit in the top panel. Values plotted as asterisks are obtained from balancing advection and diffusion at each station (assuming steady salinities, see Largier et al., 1996). In the bottom panel, residence time is plotted - values are calculated from Eq. (3).

Largier et al. (1996) find that this simple one-dimensional approach adequately represents the salinity distributions of 5 illustrative examples: San Diego Bay, Mission Bay and Tomales Bay, which are discussed in this paper, and Elkhorn Slough (California) and Langebaan (South Africa). Residence times in the hypersaline inner basin vary from 10 to 100 days.

Surface Buoyancy Fluxes

While salinity is a useful conservative tracer of water residence, to understand density structures and potential buoyancy-driven exchange, one has to consider the simultaneous changes in salinity and temperature. This is particularly true for mid-latitude west coast regions which are characterized by coastal upwelling, cool ocean waters and significant temperature gradients. In tropical systems, where the ocean is warm, temperature gradients are less important (e.g., Wolanski, 1986). In freshwater "estuaries" connected to large lakes, temperature is all important as there is no active salinity effect (e.g., Hamblin and Lawrence, 1990).

As noted, outer and middle San Diego Bay exhibits a significant temperature gradient whereas the maximum salinity gradient occurs farther into the bay. The resultant density minimum is

clearly illustrated on a temperature-salinity plot (Fig. 7). This key structure of low-inflow west coast estuaries can be illustrated with a very simple model of heating and evaporation. Bulk formulae for surface heating (e.g., Gill, 1982) can be reduced, through approximation, to a simple dependence on the time that a water parcel has been within the estuary:

$$Q = Q_{other} + \rho_a c_p D_h u(T_a - T)$$
$$= q(T_{eff} + T_a - T)$$

where T is the (surface) water temperature and T_a is atmospheric temperature; Q_{other} represents the heat flux terms other than sensible heat flux. These other heat flux terms are expected to have a much weaker dependence on the increasing surface water temperature, and are treated as constant over the time scale of interest in this simplification. They are represented by an effective constant temperature addition T_{eff} to atmospheric temperature T_a. The coefficient q is a product of air density ρ_a, heat capacity of the air c_p, wind speed u, and a dimensionless heat transfer coefficient (Stanton number) D_h. The change in temperature is then

$$\partial_t T = \frac{Q}{c_w h \rho} = b - cT$$

where

$$b = \frac{q}{c_w \rho h}\left(T_{eff} + T_a\right)$$

and

$$c = \frac{q}{c_w \rho h}$$

ρ is the water density, c_w the heat capacity of the water and h the water depth. Thus, the temperature of a parcel of water that has been resident in the basin for time t is given as

$$T(t) = \frac{b}{c} - de^{-ct} \tag{4}$$

where

$$d = \frac{b}{c} - T(t=0)$$

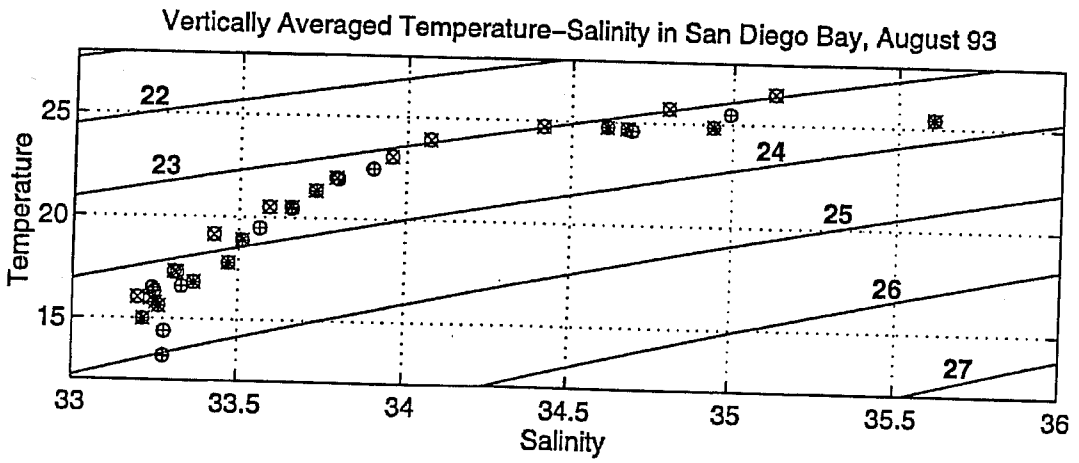

Figure 7. Vertically averaged temperature-salinity data from San Diego Bay (August 1993, see Fig. 5) plotted over a sigma-t field.

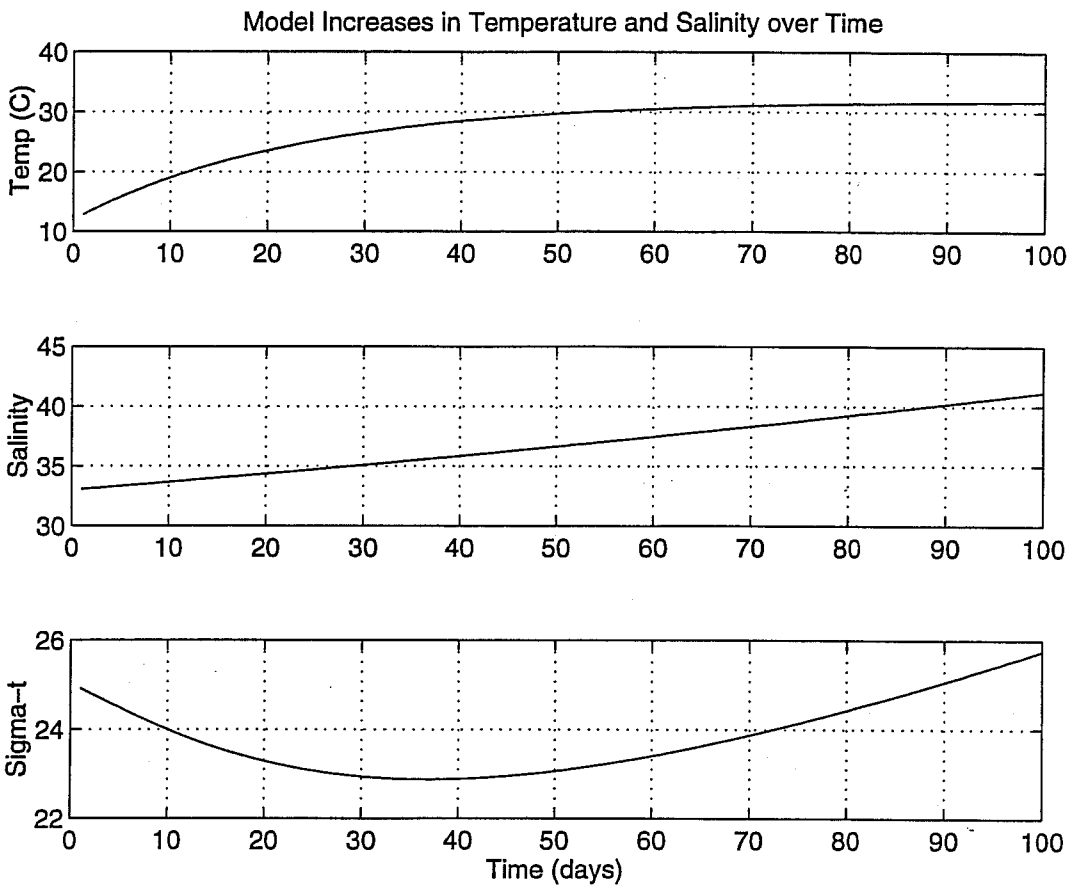

Figure 8. Model results for the increase of temperature from Eq. (4) and the increase of salinity from Eq. (5) as a function of time that a water parcel has been resident in a shallow, zero-inflow basin. Parameter values are those typical of Californian systems. The temporal decrease and subsequent increase in calculated density is shown in the bottom panel.

This gives the rate of increase in water temperature as a simple dependence on the temperature itself (assuming constant wind, air temperature, humidity, insulation and vapor pressure). The water heat content is saturated (under these constant conditions) when T increases to balance T_a+T_{eff}.

Under these conditions, evaporation occurs at an approximately constant rate, being only weakly dependent on surface temperature and salinity. Thus, the salinity of a parcel of water that has been resident in the basin for time t is given as

$$S(t) = \frac{S_0}{1 - Et/h} \tag{5}$$

Starting with ocean water of temperature 12° C and salinity 33 at time t=0 (as the parcel of water enters the shallow-water basin), and assuming conditions representative of a low-inflow California estuary, the asymptotic increase in temperature and the constant increase in salinity are plotted for a 100-day period (Fig. 8). Initially, density decreases due to warming (net negative buoyancy flux). A density minimum is noted after a time period of about a month. If the San Diego Bay data from August 1993 are plotted against residence time, given by Eq. (3), the same structure is observed (Fig. 9).

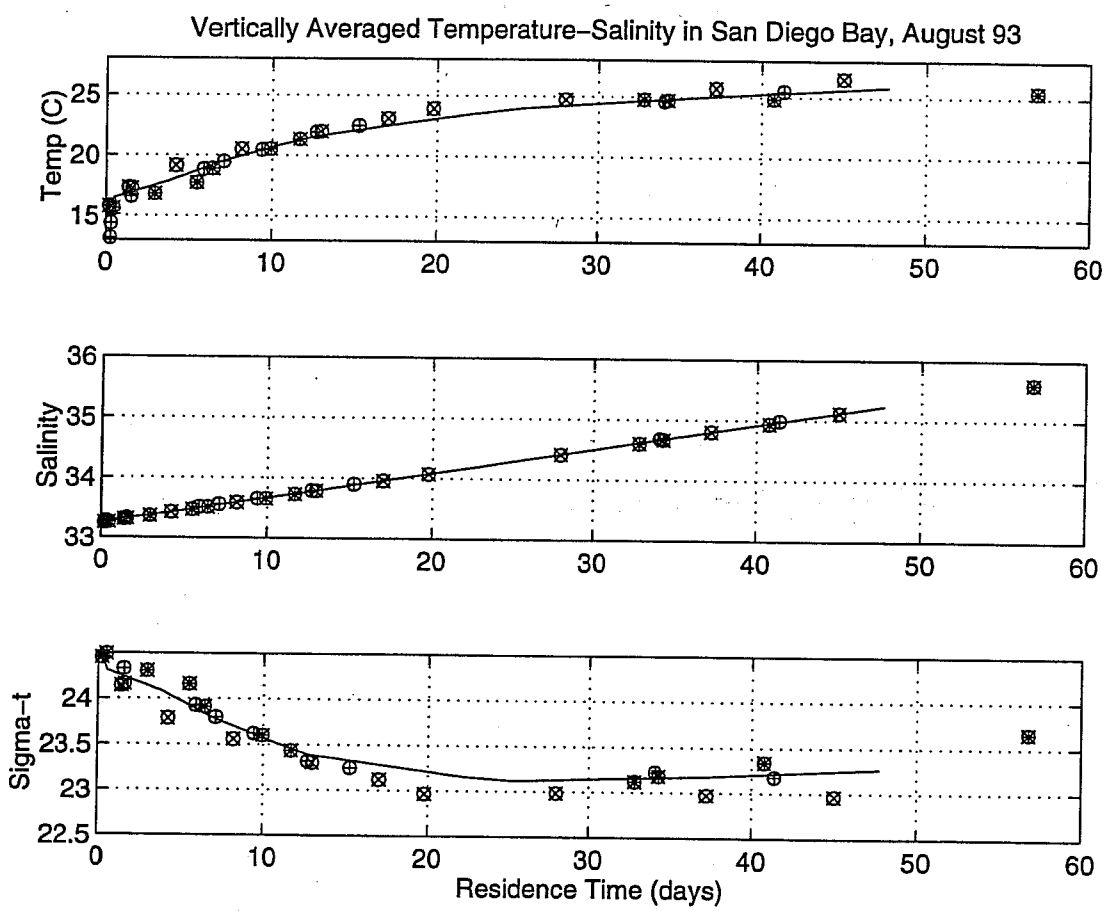

Figure 9. Observed temperature, salinity, and sigma-t values in San Diego Bay (August 1993, Fig. 5) plotted as a function of residence time, estimated from Eqn. (3).

Longitudinal Density Structure

The time history of water in a quasi-steady system is reflected in the distance of water parcels from the ocean. Water further from the ocean is older on average, as described by the one-dimensional diffusion model of these long, narrow basins. Using the solution for S(x) under the assumption of $K=kx^2$, as in Eq. (2), and estimating residence time by the degree of hypersalinity, one obtains a simplified longitudinal variation in residence time:

$$\tau_{res}(x) = \frac{h}{E}\left[1-\left(\frac{x}{L}\right)^{E/kh}\right]$$

which can be written as

$$x(\tau_{res}) = L\left[1-\frac{E\tau_{res}}{h}\right]^{kh/E} \qquad (6)$$

where x is th
simplest one-
expected spati
input and fres
obtains the lor
(Fig. 10e).

Whereve
stratified excl
salty, dense i
and Simpson
model output
outer estuary
Fig. 11). In

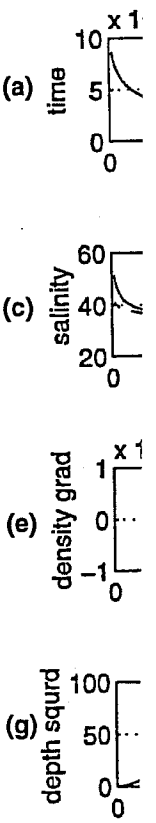

Figure 10. (
Californian L
(4). (c) Mode
The dashed li
basin shoals
temperature
(f) Illustrativ
of the estuar
dependence
and Simpson

where x is the distance from the head at which a given residence time τ_{res} would occur in this simplest one-dimensional model (Fig. 10a). Using this time-to-space conversion, one obtains the expected spatial increase in temperature and salinity due to the temporally integrated model heat input and freshwater removal (Fig. 10b, c). Further, from these $T(x)$ and $S(x)$ distributions, one obtains the longitudinal density distribution $\rho(x)$ (Fig. 10d) and the longitudinal gradient in density (Fig. 10e).

Wherever the longitudinal density gradient is strong enough, one may expect it to drive a stratified exchange flow - cold, dense seawater intruding as a basal flow near the mouth and/or salty, dense inner basin water draining seaward as a basal flow near the head. Following Linden and Simpson (1988), the buoyancy-driven diffusivity is proportional to $|\sigma_x \rho|.n$. With typical model output (Fig. 10), then, one can expect maximum buoyancy effects in the deeper thermal outer estuary and in the high-gradient hypersaline region towards the head of the estuary (Fig. 10h, Fig. 11). In contrast, simple tidal diffusivity, which is proportional to x^2, decreases strongly

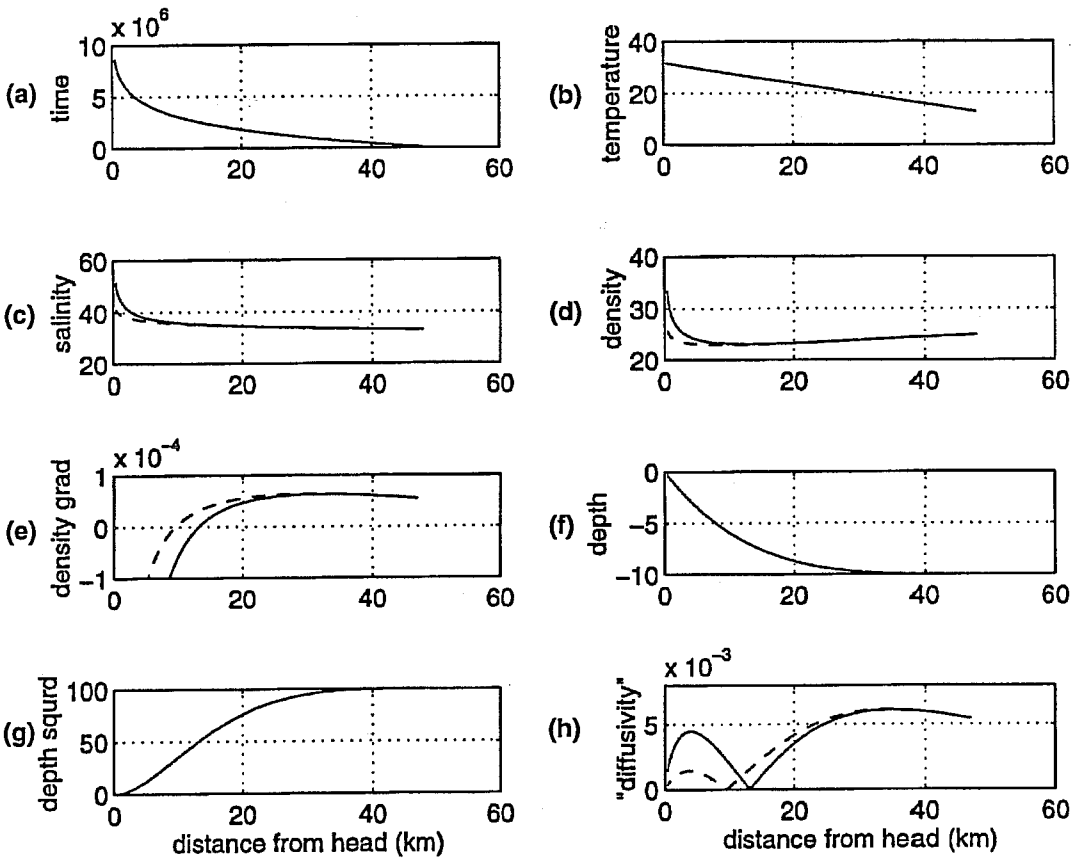

Figure 10. (a) Model residence times obtained from Eq. (6), with parameter values being typical of those in Californian LIE's. (b) Model temperature, given residence time from first panel and heating modeled by Eq. (4). (c) Model salinity, given residence time from first panel and salinity increase over time modeled by Eq. (5). The dashed line is for a constant depth basin, whereas the solid line indicates how salinity values increase if the basin shoals markedly towards the head as illustrated in panel (f). (d) Density calculated from model temperature and salinity. Solid line is for adjusted salinity (as in third panel). (e) Longitudinal density gradient. (f) Illustrative longitudinal depth profile, allowing for enhanced hypersalinity in the shallow regions at the head of the estuary. (g) The square of depth as a function of longitudinal position. (h) The typical longitudinal dependence of buoyancy diffusivity values in a low-inflow estuary, based on the dependence given by Linden and Simpson (1988). Diffusivity units are arbitrary.

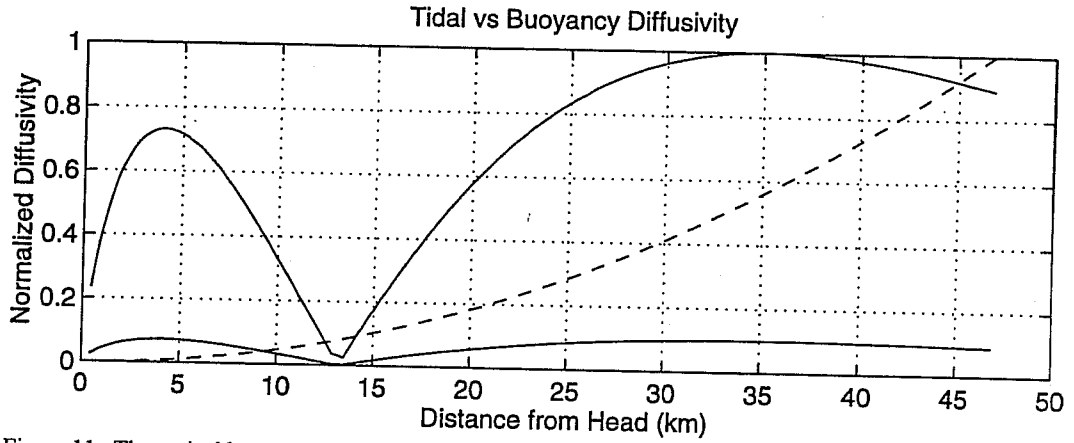

Figure 11. The typical buoyancy diffusivity profile $K \propto |\partial_x \rho|\, h^4$ for a low-inflow estuary (see solid line in Fig. 10h) compared with a typical tidal diffusivity profile $K \propto x^2$. Both diffusivities are normalized; tidal values are represented by a dashed line. An additional solid line represents the shape of buoyancy diffusivities that are an order of magnitude smaller that the tidal values. In this case, buoyancy diffusivities exceed tidal diffusivities only in the strongly hypersaline region close to the head (over the shallow region within 5-10 km from the head of this model basin).

towards the head of the basin where $x \rightarrow 0$ (Fig. 11). Thus, it is in the hypersaline region near the head of the estuary that density-driven exchange is likely to be a significant component of the longitudinal diffusion. Transient hypersaline-related inverse circulation has been observed at the landward ends of both San Diego and Mission Bays. Although weak, the observed structures are clearly due to the relaxation of the inverse density distribution. In Fig. 12, the density minimum as well as the two regions of stratified exchange flow are evident. These coherent vertical structures are transient, disappearing tidally. The detailed hydrodynamic structures of the "thermal estuary" part of San Diego Bay are discussed by Chadwick et al (1996). Aspects of the role of buoyancy exchange in Tomales Bay are addressed through a model study of historical depth changes in Tomales Bay (Hearn et al., 1996).

Strongest evaporation-associated inverse circulation is expected in deep systems, with relatively weak vertical mixing, e.g., the Mediterranean Sea (Lacombe and Richez, 1982) and Spencer Gulf (Nunes Vaz et al., 1990). However, significant inverse circulation, albeit transient, can be expected in evaporative estuaries with extensive shallows, to enhance the net evaporative loss of freshwater, and deep channels, in which density exchange flow can occur. An example is Laguna Ojo de Liebre (Fig. 12a in Postma, 1965). It appears that significant inverse circulation is also found in tidal creeks through mangrove swamps, due to the large evapotranspiration through the mangrove plants (e.g., Maputo Bay, Mocambique, A. Hoguane, pers. comm.).

Conclusion

In many mediterranean-climate, west coast estuaries one can identify up to 4 distinct hydrodynamic regimes (Fig. 13). The presence and extent of these regimes varies seasonally. Closest to the mouth, a "marine" regime is typically found. Residence times are comparable to the tidal period, temperature and salinity are similar to oceanic values and diffusivity is dominated by tidal effects, particularly tidal pumping. With increased distance from the sea (at least one tidal excursion), residence times increase to several days and significant temperature gradients are observed. This "thermal" regime is distinguished by large Q/h and it is absent in regions where the oceanic source water is warm. At longer residence times, found deeper into the basin, the heat content is saturated and an evaporative increase in salinity dominates the surface buoyancy flux (E/h is large). This is the "hypersaline" regime where inverse circulation may be observed. In

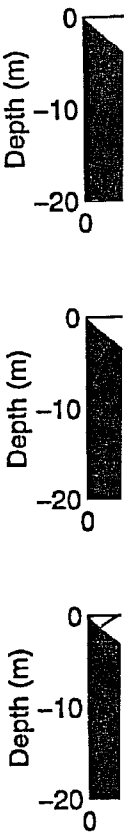

Figure 12.
August 19

some syst
dry seaso
density-d
Chadwicl
(Schwartz
paper) an
Gulf (Wo
net longit
$\partial_x \rho$ exis
as sugges
On
tends to l
estuarine
of the ba
cycle). C
the open
summer
density g
in enhan
in shallo
diffusive

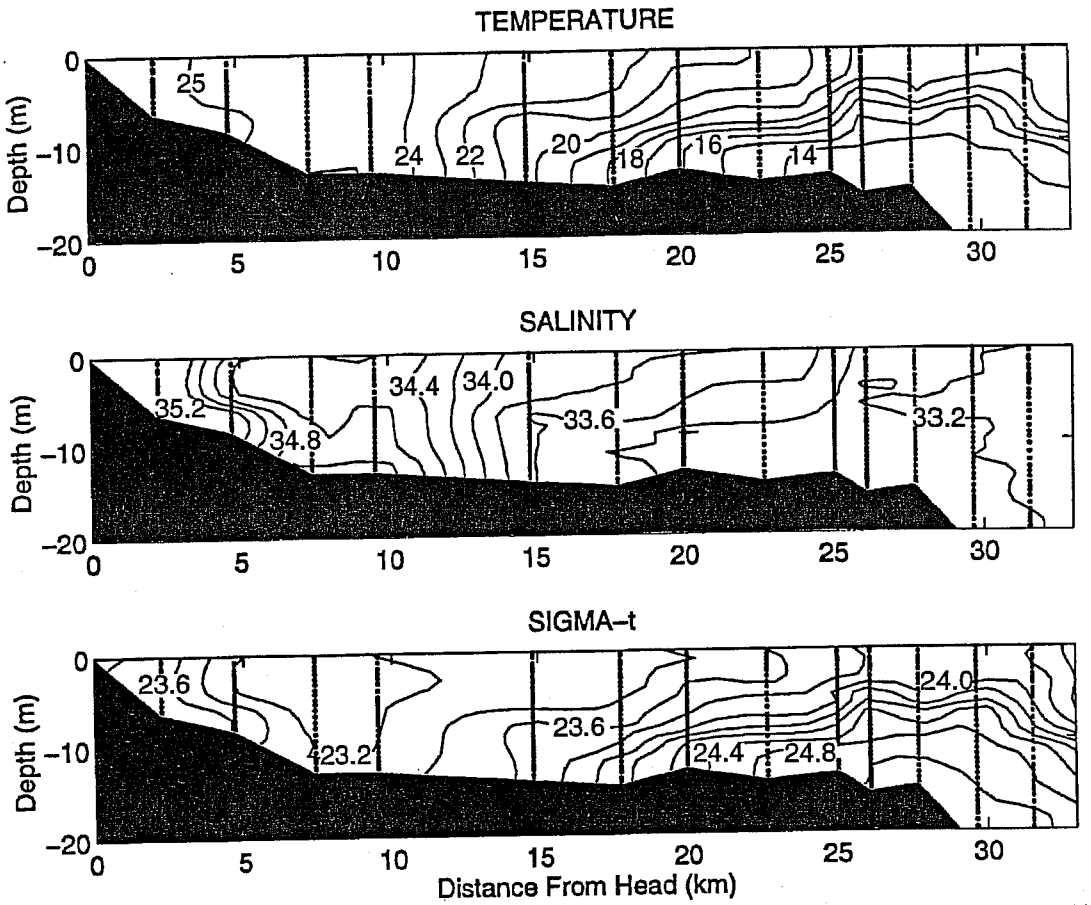

Figure 12. Vertical-longitudinal sections of temperature, salinity and sigma-t during slack highwater on 10 August 1993. Actual data points are indicated by dots (CTD profiles).

some systems, a small freshwater inflow $R << EwL$ (where L is the basin length) persists during the dry season and an "estuarine" regime may be observed at $x < R/Ew$. There is some evidence that density-driven circulation occurs in the thermal regime - e.g., San Diego Bay (this paper, and Chadwick et al., 1996), Hamilton Harbor (Hamblin and Lawrence, 1990) and Hilary Harbor (Schwartz and Imberger, 1988) - in the hypersaline regime - e.g., San Diego and Mission Bays (this paper) and Laguna Ojo de Liebre (Postma, 1965) - and in the estuarine regime - e.g., Van Diemens Gulf (Wolanski, 1986). But, it is not clear how important this transient stratified exchange is to the net longitudinal exchange in tidal basins. It is clear, however, that regions of near-zero gradient $\partial_x \rho$ exist and that these regions must be dominated by tidal action. Any closed circulation cells, as suggested by Wolanski (1986), are likely to occur in non-tidal estuaries only.

On mid-latitude west coasts, such as those of the Californias, the seasonal temperature cycle tends to lead the seasonal salinity cycle by a month or two (e.g., Tomales Bay, Fig. 3), with low estuarine salinities in spring. This is due to residual river inflow in spring, the more rapid response of the basin to heating/cooling and the delay in winter rains relative to the day length (and heat cycle). Owing to this temporal lag and the spring-summer presence of cold upwelled water along the open coast, much of a Californian estuary is characterized by a "thermal" regime in early summer and by a "hypersaline" regime in the fall. It is the interaction between these longitudinal density gradients and vertical mixing that will determine the importance of surface buoyancy fluxes in enhancing estuary-ocean exchange in low-inflow systems. A study of vertical mixing processes in shallow LIE's is desirable, given the presence of both tidal and wind stirring, as well as double diffusive salinity-temperature gradients and the potential for nocturnal overturn.

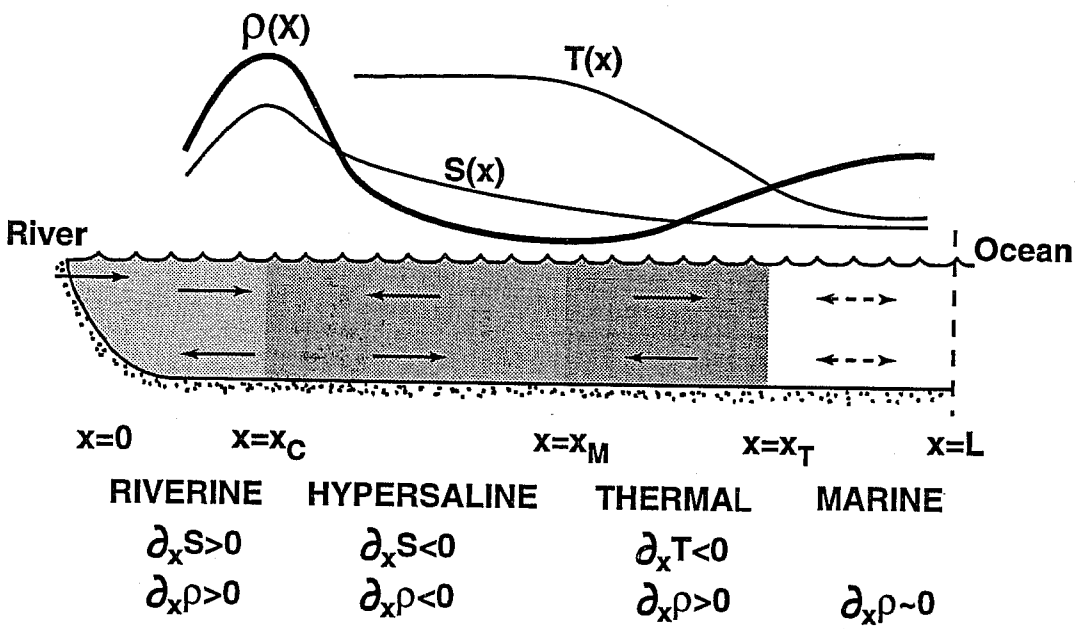

Figure 13. Schematic of the longitudinal temperature, salinity, and density profiles that may result in up to four distinct regimes in a California LIE. The marine outer basin is dominated by tidal diffusion. The thermal regime is characterized by a positive density gradient. The hypersaline regime is characterized by a negative density gradient, and the riverine regime is characterized by a positive density gradient due to river inflow. A density minimum may be observed in mid-estuary and a density maximum at or near the head of the basin (e.g., Fig. 7).

Acknowledgments. We are grateful to our colleagues, Steve Smith, Tim Hollibaugh, and Kimball Millikan, amongst others, for their part in data collection and scientific discussion. In this work, support was received from the National Science Foundation (Land Margin Ecosystem Research), Contracts 89-14833 and 89-14921; the California Department of Boating and Waterways, Interagency Agreements 91-100-080-19, 92-100-060-21, and 93-100-030-16; and the California Regional Water Quality Control Board (San Diego Region), Interagency Agreement 1-188-190-0.

References

Chadwick, D. B., J. L. Largier, and R. T. Cheng, The role of thermal stratification in tidal exchange at the mouth of San Diego Bay, Proceedings of 7th International Conference on the Physics of Estuaries and Coastal Seas, edited by D.G. Aubrey and C.T. Friedrichs, pp. (this volume), 1996.

Gill, A. E., *Atmosphere-Ocean Dynamics*. Academic Press, Oxford, 500 pp., 1982.

Hamblin, P. F., and G. A. Lawrence, Exchange flows between Hamilton Harbor and Lake Ontario, in *Proceedings of 1990 Annual Conference Canadian Society Civil Engineering*, Hamilton, May 1990, vol. 5, 140-8, 1990.

Hearn, C. J., J. L. Largier, S. V. Smith, , J. Plant, and J. Rooney, Effects of changing bathymetry on the summer buoyancy dynamics of a shallow mediterranean estuary; Tomales Bay, California, *Proceedings of 7th International Conference on the Physics of Estuaries and Coastal Seas,* edited by D.G. Aubrey and C.T. Friedrichs, pp. (this volume), 1996.

Lacombe, H., and C. Richez, The regime of the Straits of Gibraltar,in *Hydrodynamics of Semi-enlosed Seas*, edited by J. C. J. Nihoul, pp. 13-73, Elsevier, Amsterdam, 1982.

Largier, J. L., B. A. Magnell, and C. D. Winant, Subtidal circulation over the northern California shelf, *J. Geophys. Res., 98*(C10), 18147-18179, 1993.

Largier, J. L.
regions,
Lentz, S. J. (e
Oceano
Linden, P. F.,
Res., 8,
Nunes Vaz, F
Cont. Si
Postma, H., '
604, 19
Pritchard, D.
37-44,
Schwartz, R.
88-259,
Wolanski, E.
Sci., 22

Largier, J. L., J. T. Hollibaugh, and S. V. Smith, Seasonally hypersaline estuaries in mediterranean climate regions, *Est. Coast. Shelf Sci.*, in press, 1996.

Lentz, S. J. (ed.), *CODE (Coastal Ocean Dynamics Experiment). A collection of reprints*, 817 pp., Woods Hole Oceanographic Institution, Woods Hole, MA, 1991.

Linden, P. F., and J. E. Simpson, Modulated mixing and frontogenesis in shallow seas and estuaries, *Cont. Shelf Res., 8,* 1107-1127, 1988.

Nunes Vaz, R. A., G. W. Lennon, and D. G. Bowers, Physical behaviour of a large, negative or inverse estuary, *Cont. Shelf Res., 10*(3), 277-304, 1990.

Postma, H., Water circulation and suspended matter in Baja California lagoons, *Neth. J. Sea Res., 2*(4), 566-604, 1965.

Pritchard, D. W., Observations of circulation in coastal plain estuaries, in *Estuaries,* edited by G. H. Lauff, pp. 37-44, AAAS Publ. #83, Washington, 1967.

Schwartz, R. A., and J. Imberger, Flushing behaviour of a coastal marina, *Environmental Dynamics Ref.*, ED-88-259, University of Western Australia, Nedlands, Australia, 1988.

Wolanski, E., An evaporation-driven salinity maximum zone in Australian tropical estuaries, *Est. Coast. Shelf Sci., 22*, 415-424, 1986.